



HAL
open science

Structural and ferroelectric properties of $\text{Sr}_{1-x}\text{BaxBi}_2\text{Nb}_2\text{O}_9$ thin films obtained by dip-coating

Y. González-Abreu, A. Peláiz-Barranco, Pierre Saint-Grégoire, C.

Moreno-Crespo, H. Limborço, J. González

► **To cite this version:**

Y. González-Abreu, A. Peláiz-Barranco, Pierre Saint-Grégoire, C. Moreno-Crespo, H. Limborço, et al.. Structural and ferroelectric properties of $\text{Sr}_{1-x}\text{BaxBi}_2\text{Nb}_2\text{O}_9$ thin films obtained by dip-coating. *Journal of Advanced Dielectrics*, 2017, 07 (05), pp.1750035. 10.1142/S2010135X17500357. hal-04525337

HAL Id: hal-04525337

<https://hal.science/hal-04525337>

Submitted on 21 May 2024

HAL is a multi-disciplinary open access archive for the deposit and dissemination of scientific research documents, whether they are published or not. The documents may come from teaching and research institutions in France or abroad, or from public or private research centers.

L'archive ouverte pluridisciplinaire **HAL**, est destinée au dépôt et à la diffusion de documents scientifiques de niveau recherche, publiés ou non, émanant des établissements d'enseignement et de recherche français ou étrangers, des laboratoires publics ou privés.



Distributed under a Creative Commons Attribution 4.0 International License

Structural and ferroelectric properties of $\text{Sr}_{1-x}\text{Ba}_x\text{Bi}_2\text{Nb}_2\text{O}_9$ thin films obtained by dip-coating

Y. González-Abreu*, A. Peláiz-Barranco^{*§}, P. Saint-Grégoire[†], C. E. Moreno-Crespo*,
H. Limborço[‡] and J. C. González[‡]

^{*}*Facultad de Física – IMRE, Universidad de La Habana. San Lázaro y L, Vedado
La Habana 10400, Cuba*

[†]*MIPA Laboratory, University of Nîmes, Rue du Docteur Georges Salan
CS 13019, 30021 Nîmes cédex, France*

[‡]*Departamento de Física – ICEX, Universidade Federal de Minas Gerais
Belo Horizonte, MG 31270-901, Brasil
[§]pelaiz@fisica.uh.cu*

Received 6 September 2017; Revised 3 October 2017; Accepted 4 October 2017; Published 31 October 2017

The paper presents the structural and ferroelectric results for $\text{Sr}_{1-x}\text{Ba}_x\text{Bi}_2\text{Nb}_2\text{O}_9$ ($x = 0.30; 0.85$) thin films, which were obtained by using dip-coating. The solutions containing the desirable ions were prepared from the powders of the previous studied ceramic samples. The films were deposited at room temperature on Fluorine-doped Tin Oxide (FTO) substrates and submitted to a heat treatment for crystallization. The films were characterized by using scanning microscopy electronic, energy dispersive spectroscopy and ellipsometry. Hysteresis ferroelectric loops were obtained, at room temperature, by using a Sawyer-Tower circuit at several frequencies. A well-defined grain structure was observed for both compositions. The energy dispersive spectroscopy (EDS) measurements revealed the presence of the corresponding elements from the chemical composition of the ceramic systems. The band-gap energy was around 3.3 eV for both samples. Typical hysteresis loops for normal and relaxor ferroelectrics were obtained for $x = 0.30$ and 0.85, respectively.

Keywords: Ferroelectrics; Aurivillius; thin films; relaxor.

1. Introduction

The ferroelectric materials of the Aurivillius family have received great attention due to the lead-free nature, the high spontaneous polarization, the fatigue-free behavior, the relatively low processing temperatures, the high Curie temperatures and the piezoelectric properties, which made them good candidates for high-temperature piezoelectric applications and memory storage.¹⁻⁷ Its general formula is $[\text{Bi}_2\text{O}_2]^{2+}[\text{A}_{n-1}\text{B}_n\text{O}_{3n+1}]^{2-}$, where A can be Sr^{2+} , Ca^{2+} , Ba^{2+} , etc.; B can be Nb^{5+} , Ta^{5+} , W^{6+} , etc., and n is the number of corner sharing octahedral forming the perovskite-like slabs. The ferroelectricity for these systems is strongly depending on the crystallographic orientation, being the aim of continuing research.^{8,9} These have the majority polarization vector along the a-axis in a unit cell and the oxygen vacancies prefer to stay in the Bi_2O_2 layers, where their effect upon the polarization is thought to be small, and not in the octahedral site that controls polarization.

Previous studies on the $\text{Sr}_{1-x}\text{Ba}_x\text{Bi}_2\text{Nb}_2\text{O}_9$ ceramic system have showed that the increase of the barium concentration provides a transition from a normal ferroelectric ($x \leq 30$ at.%) to a relaxor behavior ($x \geq 50$ at.%), which is explained considering the mixing of different elements into A sites and

bismuth sites in the layered structure.¹⁰ On the other hand, the $\text{Sr}_{0.70}\text{Ba}_{0.30}\text{Bi}_2\text{Nb}_2\text{O}_9$ ceramic sample has showed the best piezoelectric and ferroelectric properties.¹¹ From these results, two compositions have been selected to develop thin films, one of them showing the best properties and also a normal ferroelectric–paraelectric phase transition ($x = 0.30$ at.%)^{10,11}; the other one, which exhibits a relaxor behavior ($x = 0.85$ at.%)¹⁰. The present paper shows the structural and ferroelectric results for $\text{Sr}_{1-x}\text{Ba}_x\text{Bi}_2\text{Nb}_2\text{O}_9$ ($x = 0.30; 0.85$) thin films, which were obtained by using dip-coating.

2. Experimental Procedure

The solutions containing the desirable ions were prepared from the powders of the previous studied ceramic samples, which were obtained by conventional mixed oxides method.^{10,11} The stock solutions were prepared by dissolution of the powders (0.5 g of each composition) in acid solution (10% of nitric acid (HNO_3) and 90% of distilled water). The dissolutions were optimized by heating up to around 80°C for 1 h. Both solutions were clear and transparent, showing that all elements were dissolved. The resin was obtained by the Pechiney's method using citric acid and ethylene glycol

(citric acid/ethylene glycol = 42/58 in mol.%). The mixture was heated at 70°C for 1 h, when transparent resin was obtained. After that, the resin and the stock solutions were mixed at 90°C for 1 h. The films were deposited at room temperature on Fluorine-doped Tin Oxide (FTO) substrates by using dip-coating (commercial system). Finally, the deposited films were submitted to a heat treatment of 450°C for crystallization. The deposited films were crack-free and uniform on the substrates.

X-ray diffraction measurements at room temperature did not reveal any information because the area of the deposited films was lower than that of the diameter of the beam. Almost the observed diffraction lines were associated to the FTO substrate. Morphology of grains and composition were studied by using Scanning Electron Microscopy (SEM) and Energy Dispersive Spectroscopy (EDS) by using a Quanta FEG 3D from FEI Company, USA. Spectroscopy ellipsometry measurements were performed on the samples at room temperature, in order to get the corresponding thicknesses, roughness and band-gap energy, by using a rotating compensator ellipsometer J. A. Woollam M-2000 RCE. The spectral and the angular ranges were, respectively, 245–1690 nm and 45°–80°. The measured quantities^{12,13} were the amplitude ratios for the parallel and perpendicular components of the electric field ($\tan \psi$) and the phase difference between them (Δ). These parameters were measured as function of the photon energy. The polarization (P)–electric field (E) dependences (hysteresis loops) were obtained by using a modified Sawyer-Tower circuit at room temperature and several frequencies.¹⁴

3. Results and Discussion

Figure 1 shows the SEM micrographs for the obtained thin films. A well-defined grain structure was observed for both

samples with an average grain size of 254 nm and 246 nm for SBBN-30 and SBBN-85, respectively. The EDS measurements revealed the presence of Sr^{2+} , Bi^{2+} , Ba^{2+} , Nb^{5+} and O^{2-} in correspondence with the elements from the chemical composition of the ceramic systems, which were used to obtain the thin films. Figure 2 shows the EDS spectra for the thin films. The overall content obtained for these elements is reported in Table 1. The results suggest a good correspondence with those predicted by the nominal equation. The slightly disagreement for Sr and Nb in SBBN-85 could be due to a stronger background of the C peak than that of the SBBN-30; the slightly lower content for Bi in SBBN-30 is associated to its volatilization.

Figure 3 shows the photon energy dependence for Δ and ψ for the studied thin films. It can be observed that the band-gap energy of the materials is below 3.5 eV regions, i.e., the end of the oscillations occurs near this value. From the ellipsometry measurements, the thickness, roughness and band-gap energy of the films were obtained. For that estimation, it used a model¹² considering the surface roughness, the thickness layer and the substrate. Table 2 shows the corresponding results for the studied thin films. SBBN-85 is more rugged; the band-gap energy is similar for both samples. Previous reports¹³ have showed higher values of the band-gap energy for $\text{Sr}_x\text{Bi}_y\text{Ta}_2\text{O}_9$ (between 3.98 eV and 4.25 eV) and $\text{SrBi}_2\text{Ta}_2\text{O}_9$ (4.1 eV). More recently, a band-energy gap of 2.82 eV has been reported for $\text{Bi}_4\text{Ti}_3\text{O}_{12}/\text{Bi}_2\text{Ti}_2\text{O}_7$ heterostructure nanofibers.¹⁵

Figure 4 shows the hysteresis loops for both compositions. Typical hysteresis loops for normal and relaxor ferroelectrics were obtained for SBBN-30 and SBBN-85 thin films, respectively.

For SBBN-30, it can be seen that the coercive electric field (E_C) increases with frequency as expected. The remnant polarization (P_R) has showed similar values for the higher

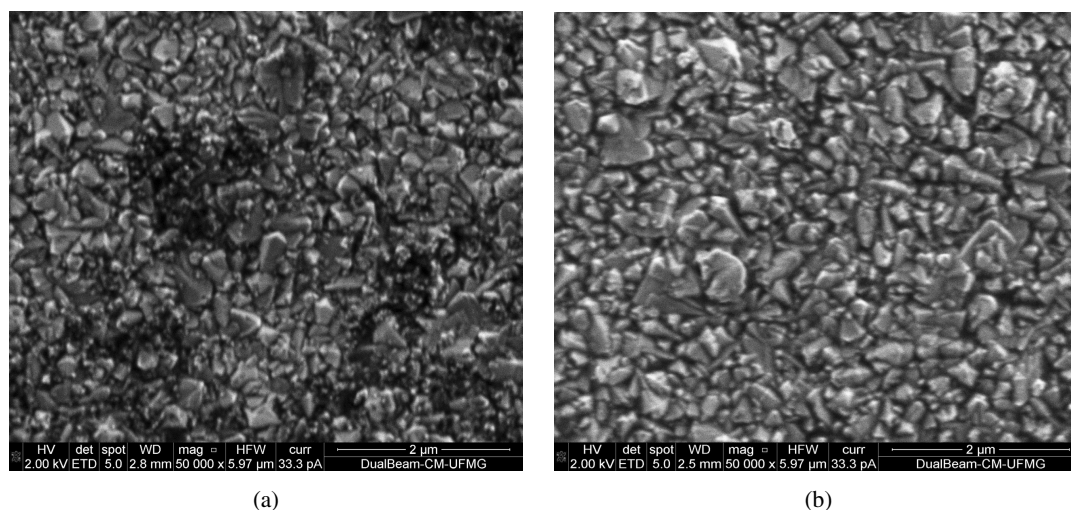


Fig. 1. SEM micrographs for the studied thin films: (a) SBBN-30, (b) SBBN-85.

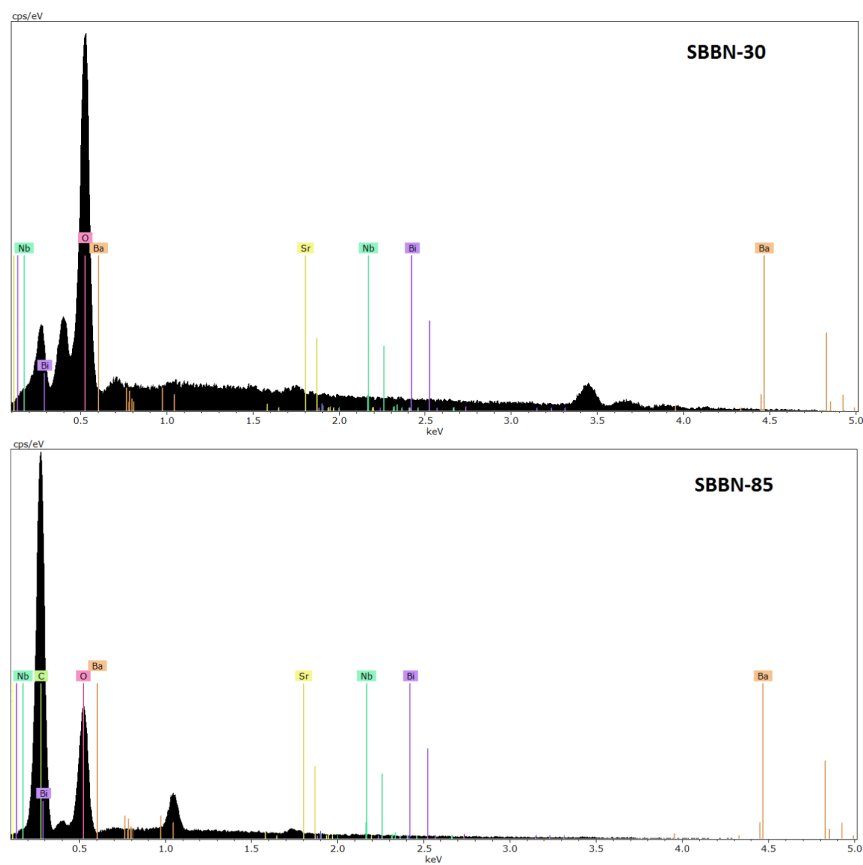


Fig. 2. (Color online) EDS spectra for the studied thin films. The color lines represent the identified elements.

Table 1. Nominal and calculated (EDS) content for the studied samples.

Thin film		Sr [%]	Ba [%]	Bi [%]	Nb [%]
SBBN-30	Nominal	14	6	40	40
	EDS	17	5	36	42
SBBN-85	Nominal	3	17	40	40
	EDS	8	18	41	33

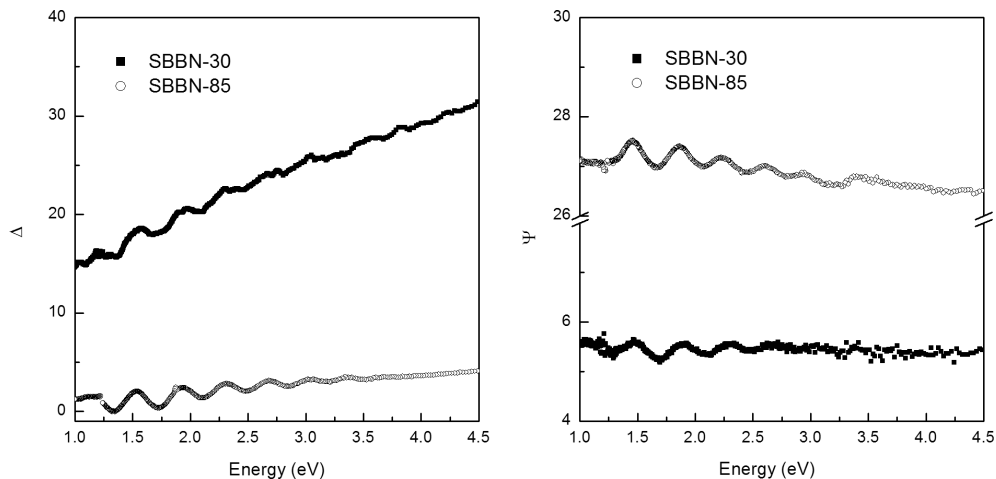


Fig. 3. Photon energy dependence for Δ and ψ .

Table 2. Thickness, roughness and band-gap energy for the studied thin films, which were obtained by using the ellipsometry measurements.

Thin film	Thickness (nm)	Roughness (nm)	Band-gap energy (eV)
SBBN-30	301 ± 1	177 ± 2	3.316 ± 0.004
SBBN-85	288 ± 2	206 ± 3	3.319 ± 0.003

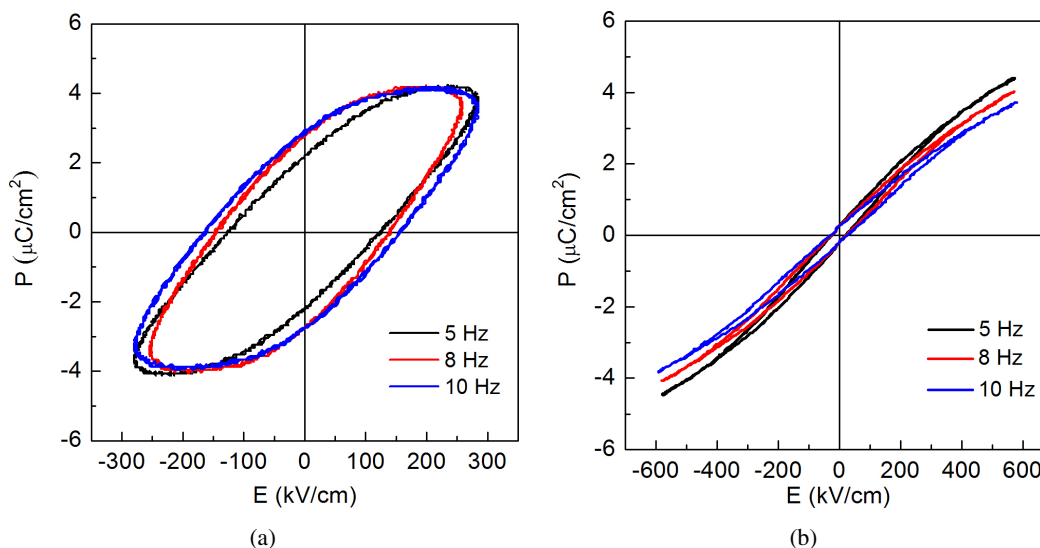


Fig. 4. Hysteresis loops, at room temperature and several frequencies, for the studied thin films: (a) SBBN-30, (b) SBBN-85.

frequencies. The sample has showed the best saturation conditions for 10 Hz, being the ratio $P_R/P_{MAX} = 0.71$ (P_{MAX} — Polarization for the maximum applied electric field). For SBBN-85, the typical slim loops show no dependence for the coercive electric field and the remnant polarization with frequency.

4. Summary

$\text{Sr}_{1-x}\text{Ba}_x\text{Bi}_2\text{Nb}_2\text{O}_9$ ($x = 0.30; 0.85$) thin films were deposited at room temperature on FTO substrates by using dip-coating. A well-defined grain structure was observed for both compositions. The EDS measurements revealed the presence of the corresponding elements from the chemical composition of the ceramic systems. The band-gap energy was around 3.3 eV for both samples. Typical hysteresis loops for normal and relaxor ferroelectrics were obtained for SBBN-30 and SBBN-85, respectively.

Acknowledgments

The authors wish to thank to the Third World Academy of Sciences (RG/PHYS/LA Nos. 99-050, 02-225 and 05-043), and to the ICTP, Trieste-Italy, for financial support of

Latin-American Network of Ferroelectric Materials (NET-43, currently NT-02). Peláiz-Barranco acknowledges to the Conseil Régional Languedoc-Roussillon for her invitation to the University of Nîmes, France. Thanks to the Embassy of France in Havana, Cuba, for financial support for the scientific cooperation between the University of Nîmes and the Havana University. The authors acknowledge the financial support from CAPES, CNPq, FINEP and FAPEMIG.

References

- P. Fang, H. Fan, J. Li and F. Liang, Lanthanum induced larger polarization and dielectric relaxation in Aurivillius phase $\text{SrBi}_{2-x}\text{La}_x\text{Nb}_2\text{O}_9$ ferroelectric ceramics, *J. Appl. Phys.* **107**, 064104 (2010).
- A. Peláiz-Barranco and Y. González-Abreu, Ferroelectric ceramic materials of the Aurivillius family, *J. Adv. Dielect.* **3**, 1330003 (2013).
- Z. Peng, Q. Chen, Y. Chen, D. Xiao and J. Zhu, Microstructure and electrical properties in W/Nb co-doped Aurivillius phase $\text{Bi}_4\text{Ti}_3\text{O}_{12}$ piezoelectric ceramics, *Mater. Res. Bull.* **59**, 125 (2014).
- Y. Zhao, H. Fan, G. Dong and Z. Liu, Enhanced electromechanical properties and conduction behaviors of Aurivillius $\text{Bi}_4\text{Ti}_{2.95}(\text{B}_{1/3}\text{Nb}_{2/3})_{0.05}\text{O}_{12}$ ($\text{B} = \text{Mg}, \text{Zn}, \text{Cu}$) ceramics, *Mater. Lett.* **174**, 242 (2016).

- ⁵U. Chon, H. M. Jang, M. G. Kim and C. H. Chang, Layered perovskites with giant spontaneous polarizations for nonvolatile memories, *Phys. Rev. Lett.* **89**, 087601 (2002).
- ⁶C. M. Raghavan, J. W. Kim, T. K. Song and S. S. Kim, Microstructural and ferroelectric properties of rare earth (Ce, Pr, and Tb)-doped $\text{Na}_{0.5}\text{Bi}_{4.5}\text{Ti}_3\text{O}_{15}$ thin films, *Appl. Surf. Sci.* **355**, 1007 (2015).
- ⁷Ch. M. Wang, J. F. Wang, S. Zhang and T. R. Shrout, Electro-mechanical properties of A-site (LiCe)-modified sodium bismuth titanate ($\text{Na}_{0.5}\text{Bi}_{4.5}\text{Ti}_4\text{O}_{15}$) piezoelectric ceramics at elevated temperature, *J. Appl. Phys.* **105**, 094110 (2009).
- ⁸H. N. Lee, D. Hesse, N. Zakharov and U. Gösele, Ferroelectric $\text{Bi}_{3.25}\text{La}_{0.75}\text{Ti}_3\text{O}_{12}$ films of uniform a-axis orientation on silicon substrates, *Science* **296**, 2006 (2002).
- ⁹T. Watanabe and H. Fuankubo, Controlled crystal growth of layered-perovskite thin films as an approach to study their basic properties, *J. Appl. Phys.* **100**, 051602 (2006).
- ¹⁰Y. González-Abreu, A. Peláiz-Barranco, J. D. S. Guerra, Y. Gagou and P. Saint-Grégoire, From normal ferroelectric transition to relaxor behavior in Aurivillius ferroelectric ceramics, *J. Mater. Sci.* **49**, 7437 (2014).
- ¹¹Y. González-Abreu, A. Peláiz-Barranco, J. D. S. Guerra and P. Saint-Grégoire, Piezoelectric behavior in $\text{Sr}_{1-x}\text{Ba}_x\text{Bi}_2\text{Nb}_2\text{O}_9$ Aurivillius-type structure ferroelectric ceramics, *Phys. Status Solidi B* **250**, 1551 (2013).
- ¹²D. Gonçalves and E. A. Irene, Fundamentals and applications of spectroscopic ellipsometry, *Quim. Nova* **25**, 794 (2002).
- ¹³J. H. Bahng, M. Lee, H. L. Park, I. W. Kim, J. H. Jeong and K. J. Kim, Spectroscopic ellipsometry study of $\text{SrBi}_2\text{Ta}_2\text{O}_9$ ferroelectric thin films, *Appl. Phys. Lett.* **79**, 1664 (2001).
- ¹⁴C. E. Moreno-Crespo, A. Peláiz-Barranco, Y. Méndez-González, A. Santana-Gil, F. Calderón-Piñar and Y. González-Abreu, Sistema experimental para el estudio de la histéresis ferroeléctrica en capas delgadas, *Rev. Cub. Fís.* **33**, 59 (2016).
- ¹⁵Y. Zhao, H. Fan, K. Fu, L. Ma, M. Li and J. Fang, Intrinsic electric field assisted polymeric graphitic carbon nitride coupled with $\text{Bi}_4\text{Ti}_3\text{O}_{12}/\text{Bi}_2\text{Ti}_2\text{O}_7$ heterostructure nanofibers toward enhanced photocatalytic hydrogen evolution, *Int. J. Hydrogen. Energy* **41**, 16913 (2016).